

## In Situ Assembly of $\text{Cu}_x\text{S}$ Quantum-Dots into Thin Film: A Highly Conductive P-Type Transparent Film

Sheng-Cong Liufu, Li-Dong Chen,\* Qin Yao, and Fu-Qiang Huang

State Key Laboratory of High Performance Ceramics and Superfine Microstructure, Shanghai Institute of Ceramics, Chinese Academy of Sciences, 1295 Dingxi Road, Shanghai, 200050, P. R. China

Received: June 8, 2008; Revised Manuscript Received: July 11, 2008

Copper sulfide ( $\text{Cu}_x\text{S}$ ) nanocrystals ranging from  $\sim 2$  to 4 nm in diameter were in situ assembled on surface-functionalized substrates at room-temperature to realize novel transparent p-type conducting film that combines good optical transparency and high electrical conductivity. The  $\text{Cu}_x\text{S}$  film exhibited superior homogeneity, highly compact microstructure and good adhesion to quartz-glass and polyethylene substrates. Results of X-ray photoelectron spectroscopy, high-resolution transmission electron microscopy and electron diffraction revealed that the film consisted of uniform fine  $\text{Cu}_7\text{S}_4$  nanocrystals with copper vacancies. Good optical transparency and large bandgap blue-shift were observed in the  $\text{Cu}_x\text{S}$  film attributed to the dominant quantum effect. The  $\text{Cu}_x\text{S}$  QD film turned out to be a p-type semiconducting film with a large conductivity up to  $10^5 \text{ S} \cdot \text{m}^{-1}$  at room temperature, which originated from the numerous defects stabilized by grain boundaries. A mechanism of the  $\text{Cu}_x\text{S}$  QD film formation has been proposed based on the surface-induced nucleation and the in situ assembly of the  $\text{Cu}_x\text{S}$  QDs.

Transparent p-type conductor in thin film form is an important material for developing optoelectronic devices such as optically transparent light-emitting diodes (LEDs), large area flat-panel displays, and solar cells. The commercial demand requires cost-efficient, flexible, and environmentally friendly materials that exhibit both high optical transmission and electrical conductivity. However, good optical transparency can be achieved but often at the expense of electrical properties, because they are interdependent and confined by semiconductor bandgap. For example, p-type transparent conducting oxides (TCO) with wide bandgaps (such as  $\text{CuAlO}_2$ ,<sup>1</sup>  $\text{CuGaO}_2$ ,<sup>2</sup> and  $x\text{ZnO} \cdot \text{Rh}_2\text{O}_3$ )<sup>3</sup> usually exhibit good optical transparencies but relatively low electrical conductivities ( $\leq 10^2 \text{ S} \cdot \text{m}^{-1}$ ). The tradeoff between transparency and conductivity motivates the search for new transparent conductors.

Bandgaps of nanocrystals can be tailored over a considerable range by varying their sizes.<sup>4</sup> Thin film composed of quantum dots (QDs) thus may offer new opportunities for realizing high-performance transparent conductor by combining the unique properties of individual QDs and the collective properties of QDs. However, to our surprise, few works have so far been reported on the preparation of conductive QDs films, especially on transparent p-type conducting QDs film. Furthermore, the assembly of QDs into conductive films (such as  $\text{CdSe}$ <sup>5</sup> and  $\text{PbTe}$ <sup>6</sup> QDs films) was typically via controlled evaporation of a preprepared concentrated nanocrystal solution onto a substrate, and hydrazine post-treatment had to be done in order to reduce the interdistance between nanocrystals for improving electrical conduction. Comparatively, in this work, a facile and practical approach is adopted to prepare QDs film by surface-induced nucleation and in situ assembly of QDs. We choose copper

sulfide ( $\text{Cu}_x\text{S}$ ) as research target for its good prospect in transparent p-type conducting film. Through manipulating ratio of nanocrystal nucleation rate to growth rate,  $\text{Cu}_x\text{S}$  QDs are stabilized in 2–4 nm to construct transparent film with high electrical conductivity. This technique provides room-temperature process, cost-efficiency and suitability for large area substrate with complex configuration and flexible plastic substrate.

Typically, quartz-glass substrates with different configurations were initially surface-functionalized by self-assembled monolayers (SAMs) of 3-(trimethoxysilyl) propylamine. Through appropriately controlling solution conditions,  $\text{Cu}_x\text{S}$  nanocrystals would be produced and in situ assembled into a homogeneous and dense  $\text{Cu}_x\text{S}$  thin film (see the Supporting Information). It should be noted that this approach is actually substrate-independent by altering suitable technique of surface modification for different substrates, e.g., using thiol SAMs for metal substrate and fumed sulfuric acid for polyethylene (PE) substrate. Photographs of optically transparent  $\text{Cu}_x\text{S}$  thin films on various substrates are shown in Figure 1a. The uniform  $\text{Cu}_x\text{S}$  films were successfully fabricated on the surfaces of quartz-glass slide, inner-wall of quartz-glass tube and flexible PE substrate. The  $\text{Cu}_x\text{S}$  film showed good adhesion to the substrates, as peel-off was not found by tape pull test. Determined by X-ray photoelectron spectroscopy (XPS), the film is composed of Cu and S elements, and the ratio of Cu/S evaluated from peak integrations is 1.45.

From the field emission scanning electron microscopy (FESEM) image in Figure 1b, it can be seen that the film is dense and homogeneous, and the inner part of the  $\text{Cu}_x\text{S}$  film is extremely continuous without any delamination or fracture. As shown in the low-magnification TEM image (Figure 1c), the film actually consists of uniform fine grains with diameter of

\* Corresponding author. E-mail: cld@mail.sic.ac.cn.

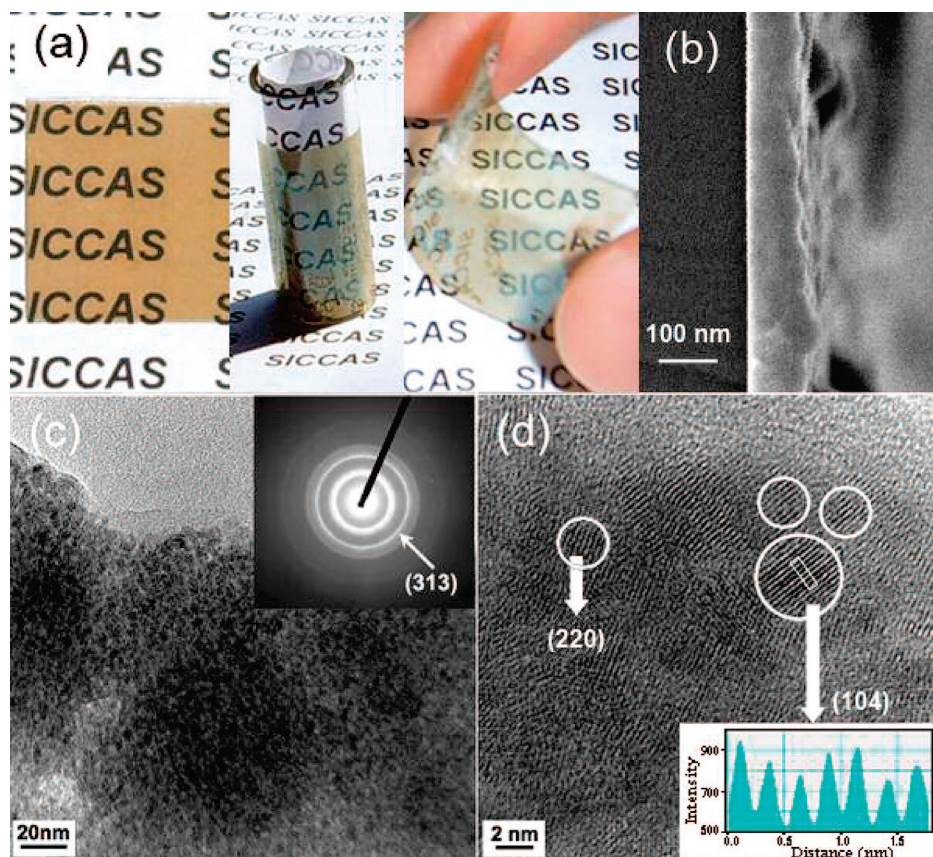


**Figure 1.** (a) Optical photographs of the  $\text{Cu}_x\text{S}$  films on quartz-glass slide, inner-wall of quartz-glass tube, and flexible PE substrate. (b) Cross-sectional SEM images of the  $\text{Cu}_x\text{S}$  film, (c) TEM, and (d) HRTEM images of the  $\text{Cu}_x\text{S}$  film on quartz-glass substrate. The inset of (c) shows the corresponding ED pattern. The inset of (d) shows the ordered structure of lattice-like lines.

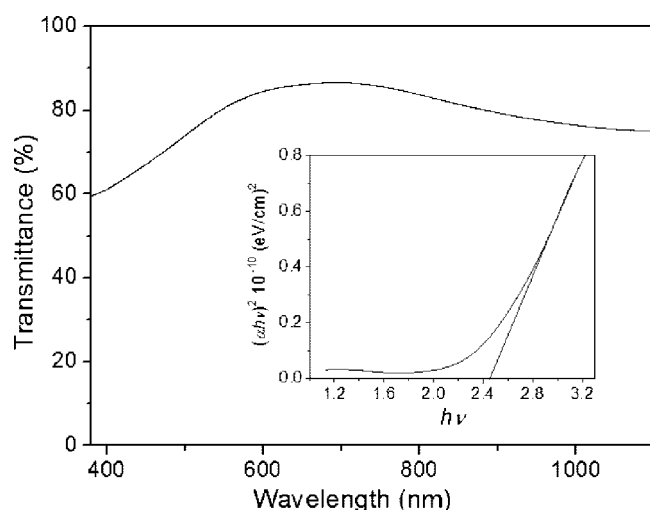


**Figure 2.** Optical transmission spectrum of the  $\text{Cu}_x\text{S}$  film on quartz-glass substrate. The inset shows the plot of  $(\alpha h\nu)^2$  against  $h\nu$  to evaluate the direct bandgap ( $E_g$ ).

about 2–4 nm, which is smaller than or comparable to the excitonic Bohr radius ( $\alpha_B$ ) of  $\text{Cu}_x\text{S}$  nanocrystals ( $\sim 4$  nm).<sup>7</sup> Electron diffraction (ED) pattern included in the inset of Figure 2c confirms the presence of nanocrystalline structure in the  $\text{Cu}_x\text{S}$  film. From the high-resolution TEM image in Figure 1d, we identify that the small grains have an ordered structure, in which the ordered spacings (0.263 and 0.280 nm) of the lattice-like structure are observed. These spacings and the plane distance (0.207 nm) determined by the sharp ring in the ED pattern can be assigned to (104), (220), and (313) planes of anilite structure, respectively. Hence we can confirm that the specific crystalline

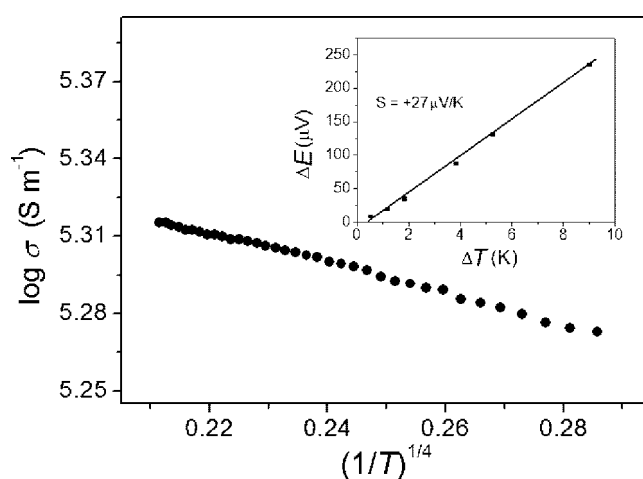


**Figure 3.** Temperature dependence of electrical conductivity of the  $\text{Cu}_x\text{S}$  film on quartz-glass slide. The inset shows the temperature difference dependence of thermoelectromotive force near room temperature.

phase of the QD is orthorhombic anilite ( $\text{Cu}_7\text{S}_4$ ), corresponding to the JPCDS Card 33–0489 file. The difference between the ratio of Cu/S (1.45) determined by XPS and the value 1.75 corresponding to the anilite crystalline phase results from the numerous copper vacancies in the  $\text{Cu}_x\text{S}$  film, which will be discussed in the later part.

Optical transmittance of the  $\text{Cu}_x\text{S}$  QD film as a function of wavelength in the range of 380–1100 nm is shown in Figure 2. The film shows an average optical transmittance above 70% in the visible region, which exceeds over the transmittances reported earlier in other  $\text{Cu}_x\text{S}$  films,<sup>8</sup> amorphous  $x\text{ZnO} \cdot \text{Rh}_2\text{O}_3$



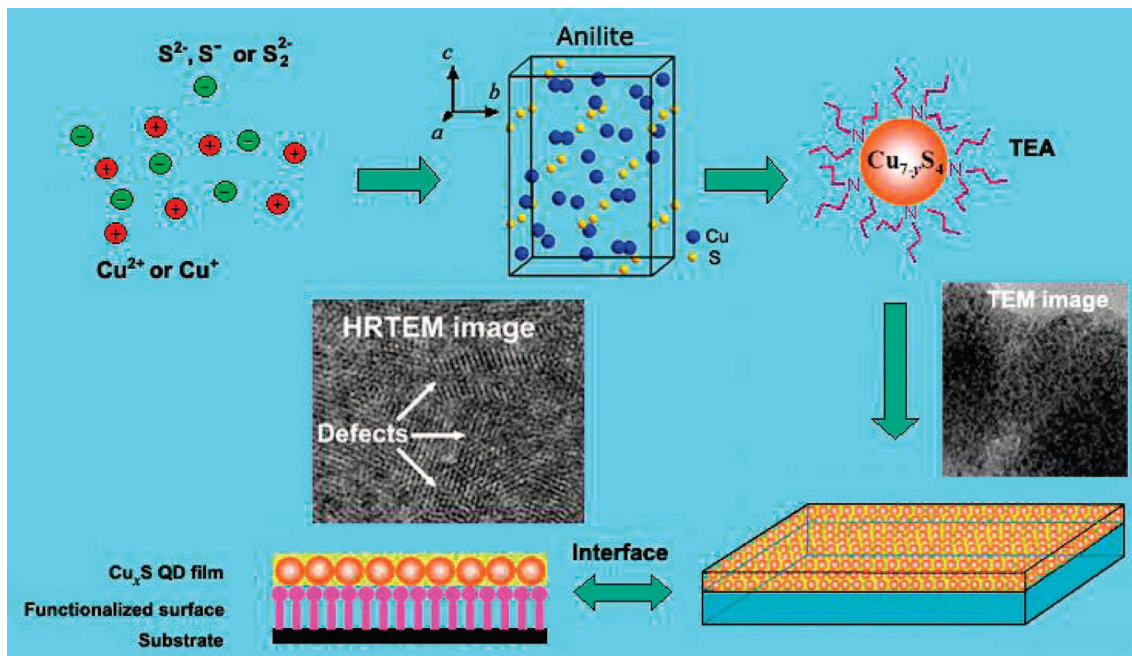


Figure 4. Scheme of mechanism of the Cu<sub>x</sub>S QD film formation.

film<sup>3a</sup> and p-type nondelafossite films (such as SrCu<sub>2</sub>O<sub>7</sub><sup>2b</sup> and LaCuOS<sup>9</sup>). The good transparency is closely related to the small grains, which minimize light absorption and scattering losses. Meanwhile, the smooth surface also reduces the light-scattering losses at the interface. The optical bandgap ( $E_g$ ) is primarily determined to be  $\sim 2.46$  eV by extrapolating the linear part of the curve to the energy axis in the inset of Figure 2. The bandgap blue-shift is evidently observed for the QD Cu<sub>x</sub>S film compared with the fundamental bandgaps of copper sulfide ( $1.2\sim 2$  eV).<sup>10</sup> Since the QD size of the Cu<sub>x</sub>S film is smaller than or comparable to the excitonic Bohr radius of Cu<sub>x</sub>S nanocrystals, it is plausible that the holes and electrons in the Cu<sub>x</sub>S film will experience a strong confinement with a characteristic reduced mass and a Coulombic interaction, and therefore resulting in the optical absorption blue-shift according to the model of the effective-mass approximation (EMA).<sup>11</sup>

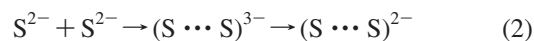
From the thermopower measurement, Seebeck coefficient of the Cu<sub>x</sub>S QD film is found to be positive ( $+27$   $\mu\text{V/K}$  at room temperature, as shown in the inset of Figure 3), confirming p-type conduction. The carrier concentration ( $n$ ), mobility ( $\mu$ ), and electrical conductivity ( $\sigma$ ) of the Cu<sub>x</sub>S film were determined by Hall measurement in the van der Pauw configuration. The electrical conductivity increases with increasing temperature ( $T$ ) (see Figure 3), indicating the semiconducting behavior from 150 to 480 K. An approximate linear relationship of the plot of  $\log \sigma$  vs  $(1/T)^{1/4}$  reveals that hopping conduction appears in the Cu<sub>x</sub>S QD film. The values of  $\sigma$ , carrier mobility ( $\mu$ ), and carrier concentration ( $n$ ) at 300 K are  $2.01 \times 10^5$  S $\cdot\text{m}^{-1}$ ,  $1.52$  cm<sup>2</sup> $\cdot\text{V}^{-1}\cdot\text{s}^{-1}$ , and  $8.26 \times 10^{21}$  cm<sup>-3</sup>, respectively. Besides exhibiting good optical transparency, the Cu<sub>x</sub>S film prepared in this work also possesses high electrical conductivity, which is 2~6 orders magnitude larger than those of other transparent p-type films at near room-temperature, such as CuMO<sub>2</sub> ( $M = \text{Al, Ga, In, etc.}$ ),<sup>1,2</sup>  $x\text{ZnO}\cdot\text{Rh}_2\text{O}_3$ ,<sup>3a</sup> and LaCuOCh ( $\text{Ch} = \text{chalcogen}$ ).<sup>9,12</sup> The high electrical conductivity originates from the large carrier concentration that is associated with the chemical composition and the microstructure of the Cu<sub>x</sub>S film.

Synthesis of the Cu<sub>x</sub>S thin film is based on the releases of copper and sulfur ions from the precursor solution. Initially,

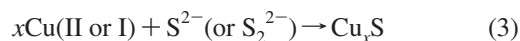
cupric chloride can form complex with ammonia,<sup>13</sup> which control the copper ion concentration. Under alkaline condition, S<sup>2-</sup> ions are produced from thiourea through the hydrolysis as following:



The high pH value of the precursor solution promotes the production of S<sup>2-</sup> ions, which then come through a sequential oxidation to form S<sub>2</sub><sup>2-</sup> groups:<sup>14</sup>



A corresponding reduction reaction takes place, leading to the conversion of Cu(II) to Cu(I). Such conversion can be visually observed via a simple color change of the precursor solution from blue to aqua color. Copper sulfide (Cu<sub>7</sub>S<sub>4</sub>) solid phase would nucleate in the form of Cu (II or I) + S<sup>2-</sup> (or S<sub>2</sub><sup>2-</sup>) when the supersaturation degree of precursor solution is so sufficiently high that the product of ions concentrations exceeds the solubility of copper sulfide phase ( $K_{\text{sp}}$ )



Although copper hydroxide or hydrated copper oxide could occur for the presence of hydroxide ions, they would spontaneously convert to copper sulfide due to the low  $K_{\text{sp}}$  of Cu<sub>x</sub>S, which consequently results in the Cu<sub>x</sub>S film without other copper compound impurities. The Cu-NH<sub>3</sub> complex that suppresses the release of free copper ions and the alkaline condition that promotes the generation of sulfur ions induce the formation of copper vacancies (Cu<sub>7-y</sub>S<sub>4</sub>), which lead to the p-type conduction of the QD film.

In the supersaturated solution, functionalized surface can reduce the nucleation barrier of copper sulfide and acts as nucleation sites due to its capacity to bind copper ions. The heterogeneous nucleation thus tends to take place at the interface between the substrate and the precursor solution. The microstructure of the Cu<sub>x</sub>S QD film depends on the film deposition process, which involves two aspects: the process of nucleus formation and the process of crystal growth. The ratio between

rates of these two processes is of fundamental importance for the  $\text{Cu}_x\text{S}$  crystal size. The supersaturation degree of the precursor solution is high for the alkaline condition, thus the rate of nucleation increases exponentially. Meanwhile, the strong complexing ability of triethanolamine (TEA) for sulfide would lead to the adsorption of TEA molecules on the Cu sites of the growing crystals, acting as capping agents and preventing their further growth. The rate of the crystal growth is expected to be greatly lower than that of the nucleation. The crystals are consequently stabilized in diameter of  $\sim 2\text{--}4$  nm. The heterogeneous nucleation incessantly takes place at the interface, and the as-formed nanocrystals are in situ assembled into a highly compact film (see Figure 4). The defects in the nanocrystals can be effectively stabilized by the numerous grain boundaries. Therefore, considerable holes occur in the  $\text{Cu}_x\text{S}$  QD film and enable its carrier concentration to reach  $10^{21}\text{ cm}^{-3}$ . The high carrier concentration not only results in the good electrical conductivity, but also leads to the Burstein–Moss shift of the bandgap toward the blue region.<sup>15</sup>

In summary, we have successfully prepared novel transparent p-type conducting film through design and assembly of quantum-dots using a simple chemical method at room temperature.  $\text{Cu}_x\text{S}$  QDs with size about  $2\sim 4$  nm in diameter are in situ assembled to the highly compact, homogeneous and well-adherent  $\text{Cu}_x\text{S}$  film that combines good optical transparency and high electrical conductivity. Numerous defects in the nanocrystals stabilized by the grain boundaries contribute to the high electrical conductivity up to  $10^5\text{ S}\cdot\text{m}^{-1}$ . This method is substrate-independent and suitable for mass production, permitting fast, cheap, and safe-deposition of large-area sulfide film. The  $\text{Cu}_x\text{S}$  QD film extends its tremendous application possibilities in transparent electronic circuits, even on flexible or complex-configuration substrates.

**Acknowledgment.** Financial support from the National Natural Science Foundation of China (Grant Nos. 50325208 and 50702069) is gratefully acknowledged.

**Supporting Information Available:** Experimental details for the synthesis of  $\text{Cu}_x\text{S}$  QD thin film. This material is available free of charge via the Internet at <http://pubs.acs.org>.

## References and Notes

- (1) Kawazoe, H.; Yasukawa, M.; Hyodo, H.; Kurita, M.; Yanagi, H.; Hosono, H. *Nature* **1997**, *389*, 939.
- (2) (a) Yanagi, H.; Kawazoe, H.; Kudo, A.; Yasukawa, M.; Hosono, H. *J. Electroceram.* **2000**, *4*, 407. (b) Sheng, S.; Fang, G.; Li, C.; Xu, S.; Zhao, X. *Phys. Stat. Sol. A* **2006**, *203*, 1891.
- (3) (a) Narushima, S.; Mizoguchi, H.; Shimizu, K.; Ueda, K.; Ohta, H.; Hirano, M.; Kamiya, T.; Hosono, H. *Adv. Mater.* **2003**, *15*, 1409. (b) Kamiya, T.; Narushima, S.; Mizoguchi, H.; Shimizu, K.; Ueda, K.; Ohta, H.; Hirano, M.; Hosono, H. *Adv. Funct. Mater.* **2005**, *15*, 968.
- (4) (a) Poznyak, S. K.; Talapin, D. V.; Shevchenko, E. V.; Weller, H. *Nano Lett.* **2004**, *4*, 693. (b) Neogi, A.; Morkoç, H.; Kuroda, T.; Tackeuchi, A.; Kawazoe, T.; Ohtsu, M. *Nano Lett.* **2005**, *5*, 213.
- (5) Dong, Y.; Wang, C.; Guyot-Sionnest, P. *Science* **2003**, *300*, 1277.
- (6) Urban, J. J.; Talapin, D. V.; Shevchenko, E. V.; Murray, C. B. *J. Am. Chem. Soc.* **2006**, *128*, 3248.
- (7) (a) Klimov, V. I.; Karavanskii, V. A. *Phys. Rev. B* **1996**, *54*, 8087. (b) Klimov, V. P.; Bolivar, H.; Kurz, H.; Karavanskii, V.; Krasovskii, V.; Korkishko, Y. *Appl. Phys. Lett.* **1995**, *67*, 653.
- (8) (a) Pathan, H. M.; Sesai, J. D.; Lokhande, C. D. *Appl. Surf. Sci.* **2002**, *202*, 47. (b) Nair, P. K.; Cardoso, J.; Dsza, O. G.; Nair, M. T. S. *Thin Solid Films* **2001**, *401*, 243. (c) Cardoso, J.; Dsza, O. G.; Ixtlilco, L.; Nair, M. T. S.; Nair, P. K. *Semicond. Sci. Technol.* **2001**, *16*, 123.
- (9) Ueda, K.; Inoue, S.; Hirose, S.; Kawazoe, H.; Hosono, H. *Appl. Phys. Lett.* **2000**, *77*, 2701.
- (10) Marshall, R.; Mitra, S. S. *J. Appl. Phys.* **1965**, *36*, 3882. (b) McLeod, P. S.; Partain, L. D.; Sawyer, D. E.; Peterson, T. M. *Appl. Phys. Lett.* **1984**, *45*, 472. (c) Gurin, V. S.; Prokopenko, V. B.; Alexeenko, A. A.; Frantskevich, A. V. *J. Mater. Chem.* **2001**, *11*, 149.
- (11) (a) Kayanuma, Y. *Phys. Rev. B* **1988**, *38*, 9797. (b) Brus, L. E. *J. Chem. Phys.* **1984**, *80*, 4403. (c) Barik, S.; Srivastava, A. K.; Misra, P.; Nandedkar, R. V.; Kukreja, L. M. *Solid State Commun.* **2003**, *127*, 463.
- (12) Ueda, K.; Hiramatsu, H.; Hirano, M.; Kamiya, T.; Hosono, H. *Thin Solid Films* **2006**, *496*, 8.
- (13) Jiang, X. C.; Xie, Y.; Lu, J.; He, W.; Zhu, L. Y.; Qian, Y. T. *J. Mater. Chem.* **2000**, *10*, 2193.
- (14) Patrick, R. A. D.; Mosselmanns, J. F. W.; Charnock, J. M.; England, K. E. R.; Helz, G. R.; Garner, C. D.; Vaughan, D. J. *Geochim. Cosmochim. Acc.* **1997**, *61*, 2023.
- (15) Suda, T.; Kakishita, K. *J. Appl. Phys.* **2006**, *99*, 076101.

JP805029W